Influence of Arrhythmias on Gated SPECT Myocardial Perfusion and Function Quantification

Kenneth Nichols, Sharmila Dorbala, E. Gordon DePuey, Siu-Sun Yao, Atul Sharma and Alan Rozanski

Columbia University College of Physicians and Surgeons and Division of Cardiology, Department of Medicine, and Division of Nuclear Medicine, Department of Radiology, St. Luke's-Roosevelt Hospital, New York, New York

Despite the importance of R-wave gating myocardial perfusion tomography for ventricular function assessment, neither prevalence of gating errors nor their influence on quantified cardiac parameters has been studied. **Methods:** Arrhythmia-induced anomalies in curves of counts versus projection angle for each R-wave segment were detected visually and algorithmically. Arrhythmia prevalence was tabulated for 379 patients (group 1) with prospective coronary artery disease (mean age 63 ± 13 y, 47% male). Myocardial counts were analyzed from all reconstructed cinematic midventricular slices to assess arrhythmia effects on percentage of systolic count increase, generally assumed to equal percentage of wall thickening. In a separate retrospective analysis of 41 patients (group 2), with coronary artery disease (mean age 64 ± 12 y, 68% male) having no significant arrhythmias, 36 of whom also underwent equilibrium radionuclide angiography, original projection data were altered to simulate arrhythmia-induced aberrant count patterns to evaluate effects on ventricular function and perfusion measurements. **Results:** Group 1 patients consisted of 26% without gating errors, 32% with count losses only in the last R-wave interval due to inconsistent transient increase of heart rate, 24% with count decreases in several late intervals due to consistently variable rates, 8% with early interval count increases paired with late interval count decreases due to ectopic beats and 9% with erratic count changes due to atrial fibrillation. Observed count patterns were strongly associated ($P < 10^{-3}$) with arrhythmias detected by electrocardiogram monitoring. In group 2 simulations, ventricular volumes changed by only 2% ± 9% and ejection fraction (EF) by only 1% ± 4% from control values and correlated linearly ($r \geq 0.96$) with control values for all simulated arrhythmias. SPECT and equilibrium radionuclide angiography EFs correlated similarly ($r = 0.85$–0.89) for control and all simulations. Percentage changes from control in perfusion defect extent and severity were larger than processing reproducibility limits, the largest change being for atrial fibrillation. Control wall thickening was 38% ± 17%, significantly lower ($P < 10^{-6}$) than for simulated arrhythmias, reflecting similar observations for group 1 patients. **Conclusion:** Even though ventricular volumes and EFs were affected minimally by arrhythmias, both perfusion analysis and wall thickening were compromised. Consequently, quality assurance of gating may be critically important for obtaining accurate quantified parameters.

Received Jun. 22, 1998; revision accepted Oct. 7, 1998.

For correspondence or reprints contact: Kenneth Nichols, PhD, Division of Cardiology, Columbia University, 622 W. 168th St., New York, NY 10032.

Key Words: gated SPECT; arrhythmias; function; perfusion; quality assurance

J Nucl Med 1999; 40:924–934

Use of R-wave gating with myocardial perfusion tomography (*1*) has become a routine diagnostic tool, permitting computation of left ventricular (LV) ejection fraction (EF) (*2,3*) and volumes (*4*) and enhancing specificity by discriminating artifacts from genuine fixed defects (*5*). Quality assurance of scintigraphic tomograms is necessary for optimal results (*6*), but in the 10 y since the introduction of gated SPECT (*1*), gating errors have received little attention, so that prevalence of arrhythmias and their effect on function and perfusion measurements have not been studied.

This causes concern because gated tomograms usually are summed into a single dataset, with the assumption that summed tomograms are the same as those collected without gating. However, some arrhythmias produce "flickering" in cinematic displays of rotating summed projection images, indicating that count inconsistencies at different projections have been introduced. Flickering of summed tomograms emulates disruption of signals from detector to computer (*7*), and backprojecting inconsistent data can result in pronounced perfusion artifacts (*8*). Because summed polar perfusion maps can aid in the detection of myocardial scar and ischemia, it is important to ascertain whether gating errors compromise perfusion quantitation. Furthermore, gated SPECT EF algorithms rely on finding myocardial shapes from perfusion images and on accurate percentage of systolic count increase as a measure of wall thickening (*9*).

To address these issues, this investigation identified common gating errors and analyzed their origin, prevalence and effects on quantified LV volumes, EF, wall thickening and myocardial perfusion.

MATERIALS AND METHODS

Study Populations

All patients were studied for routine evaluation of coronary artery disease and comprised two groups: Group 1 consisted of 379 randomly selected patients (mean age 63 ± 13 y, 47% male) analyzed prospectively to assess the prevalence of different types

of arrhythmias; group 2 consisted of 41 patients (mean age 64 ± 12 y, 68% male) analyzed retrospectively with no evidence of significant gating errors. Group 2 data were artificially altered to simulate gating errors to determine the influence of arrhythmias on cardiac parameters. Thirty-six group 2 patients also underwent equilibrium radionuclide angiography (ERNA) within 1 wk of gated SPECT studies, with no intervening change in cardiac status, or surgical or medical intervention, thereby enabling independent EF comparisons.

Gated SPECT Data Acquisition

^{99m}Tc-sestamibi stress injections were performed during peak exercise of a Bruce treadmill protocol or intravenous pharmacological coronary vasodilatation with dipyridamole (0.142 mg/kg/min infused over 4 min) using 1.11 GBq (30 mCi) for a 1-d protocol or 814 MBq (22 mCi) for a separate-day protocol (*10*). Tomograms (64 × 64, pixel size 6.4 mm) were acquired with high-resolution collimation for 20 s/projection for 64 projections over 180° with biplane detectors (General Electric "Optima"; General Electric Medical Systems, Inc., Milwaukee, WI) angled at 90°. Perfusion tomograms were acquired gated at 8 frames per R-R interval 30 min post stress. Data were included for incoming R-waves between 50%–150% of the average heart rate computed from the 10 heart beats just before commencement of data acquisition.

Gated SPECT Analysis

Butterworth (cutoff 0.40, power 10.0) prefilters, quantitative ramp x-filtering (*11*), interslice spatial averaging and time-filtering among gated frames (weighted as 1:3:1) were performed for each stress study. Stress gated projections also were summed and reconstructed with a Butterworth filter (cutoff 0.55, power 10.0). Summed stress tomograms were read visually for myocardial hypoperfusion and were compared with rest images to determine whether defects were reversible or fixed. Polar perfusionmaps were constructed from short-axis images, including calculation of abnormality "extent" (number of pixels labeled as abnormally underperfused) and "severity" (number of pixels labeled as abnormal and weighted by the excess number of SDs below gender-matched normal perfusion) (*12*). Data were reanalyzed several months after initial processing to determine reproducibility of perfusion parameters.

Algorithms previously described (*13*) were applied to paired reoriented midventricular vertical long axis (VLA) and horizontal long axis (HLA) cinematic tomograms for automated computation of ventricular volumes and EF. This included identification of end-diastole (ED) and end-systole (ES) by finding the frame numbers corresponding to minimum and maximum myocardial counts, from partial volume effects (*9*). Of relevance to this investigation, endocardial borders were derived using frames individually normalized to the same maximum counting rate. Originally, this choice was made to facilitate manual drawings of endocardial borders (*2*) and was retained when manual processing steps were automated (*13*), in the expectation that this choice would lessen the influence of gating errors on EF calculations.

When deemed necessary, an observer corrected ED and ES frame numbers to correspond to the visual impression of greatest and least LV volumes and altered manually the automated edges to conform to the visual impression of endocardia; the latter usually was necessary for cases of hypoperfused septa, or inferior walls, in

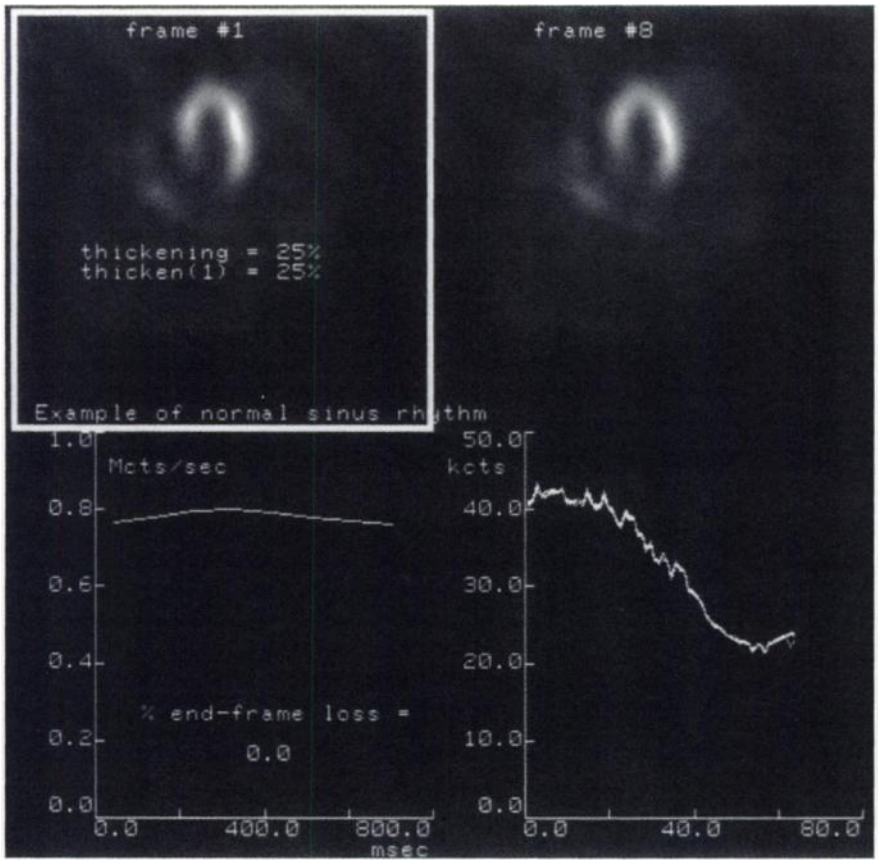

FIGURE 1. Example of standard quality assurance screen for patient in normal sinus rhythm. First (upper left) and last interval (upper right) of eight R-R intervals of mid-LV HLA cinematic tomogram is shown. Also (upper left) computed is myocardial wall thickening ("thickening") and "thicken (1)," wall thickening computed with first interval regardless of which cinematic frame contains minimum myocardial counts. (Lower left) Total mid-LV HLA counts per R-R interval are graphed, along with end-frame count loss. (Lower right) Superimposed are eight curves of total counts per projection numbers from 1 to 64, where projection 1 corresponds to the right anterior oblique 45° view and projection 64 corresponds to left anterior oblique 45° view.

conjunction with high counts in the right ventricle or hepatobiliary tract, respectively (*13*). Paired VLA and HLA endocardial outlines were combined to compute LV volumes and EFs through Simpson's rule summation (*2*), analogous to echocardiographic biplane ventricular modeling (*14*).

Equilibrium Radionuclide Angiography

ERNA studies were acquired for 36 group 2 patients who also underwent gated SPECT studies. Average ERNA administered activity was 740 MBq (20 mCi) ^{99m}Tc in vitro-labeled red blood cells. Data were acquired gated at 24 frames per R-R interval in the approximate left anterior oblique 45° projection with caudal tilt to optimize separation of heart chambers. Low-energy general-purpose collimation was used, and data were acquired for 10 min as 64 × 64 matrices with a pixel size of 3.1 mm. All ERNA data were analyzed independently of gated SPECT EF determinations by previously validated semiautomated algorithms (*15,16*).

Arrhythmia Detection

Curves of total counts versus projection angle of the eight planar images, corresponding to each segment of the R-wave interval, were evaluated visually to identify gating errors due to heart rate variability; these total counts usually were composed primarily of activity from the hepatobiliary tract. For patients in sinus rhythm, these 8 curves superimposed identically, with maxima near left

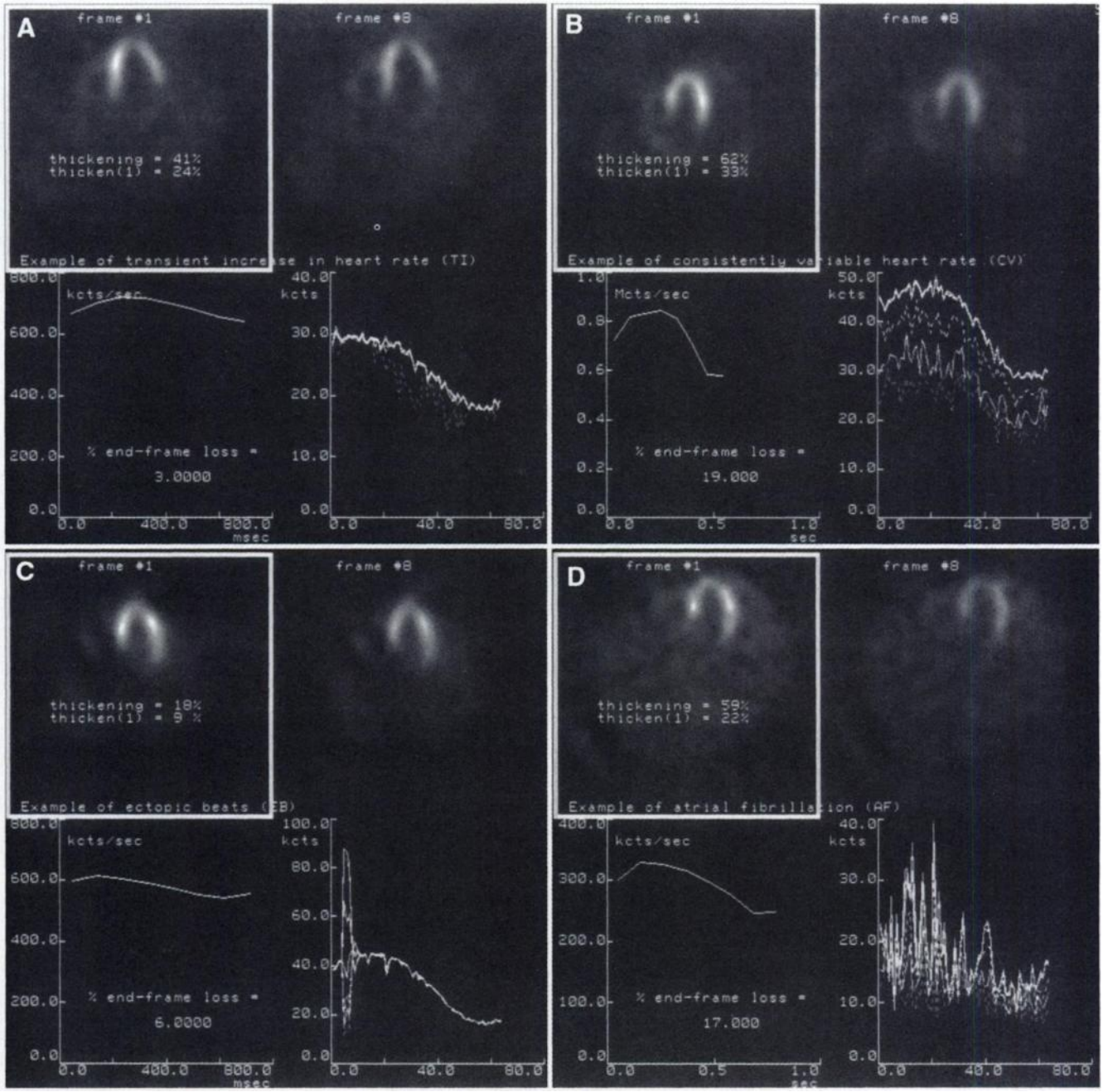

FIGURE 2. Examples of standard quality assurance screens for patients with transient increase in heart beat (A), consistently variable heart beats (B), ectopic beats (C) and atrial fibrillation (D).

anterior oblique and minima near left posterior oblique projections because of patients' self-attenuation (Fig. 1). On the basis of unusual count patterns associated with nonsinus rhythms recorded on electrocardiogram (ECG) strips during stress testing in 30 pilot studies, five categories of gating errors were defined:

1. Sinus rhythm, with insignificant deviations among curves 1–8 (Fig. 1).
2. Transient increase of heart rate, with transient count decreases only in frame 8 (Fig. 2A).
3. Consistently variable heart rates, with several late interval curves lying below and parallel to early interval curves (Fig. 2B).
4. Ectopic beats (atrial or ventricular) or transient tachycardia, bigeminy or trigeminy, with early interval count increases paired with late interval count decreases for a few curve points (Fig. 2C).
5. Atrial fibrillation, with abrupt chaotic count changes within and among curves (Fig. 2D).

Algorithms were devised to recognize these curve patterns automatically. The algorithmic definitions for detecting the above five categories included specifications as to the amount of count deviations from summed curves and the percentage of curve points having aberrant counts and were derived from the 30 pilot studies.

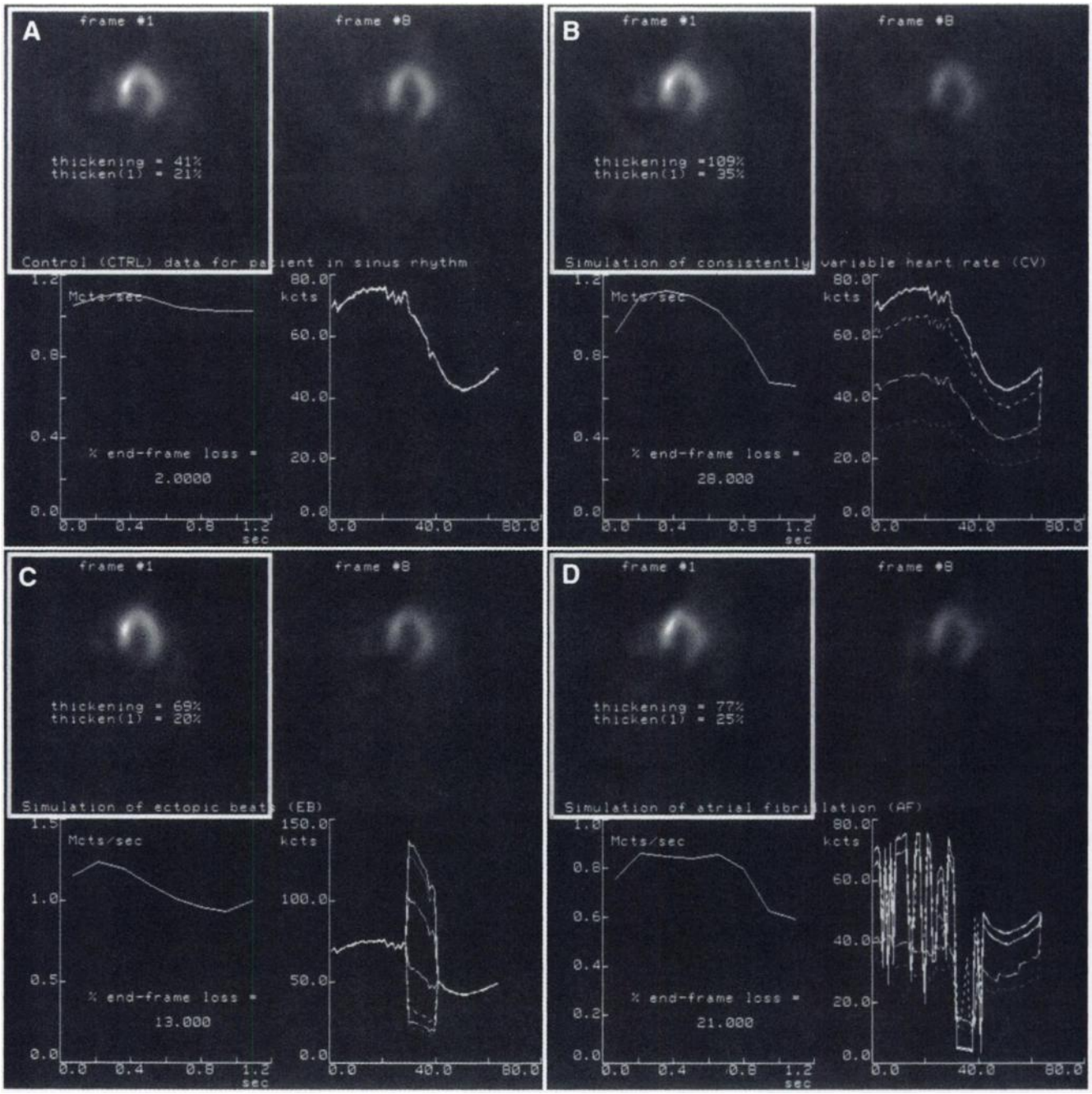

FIGURE 3. Examples of standard quality assurance screens for control data (A) and for simulations of consistently variable heart rate (B), ectopic beats (C) and atrial fibrillation (D).

Two observers categorized arrhythmias on the basis of observed curve patterns (Figs. 1 and 2) and tabulated three count change parameters computed using counts sampled from mid-HLA cinematic tomograms:

1. End-frame count loss = % [(frame 1 − frame 8)/frame 1] total counts. For patients in sinus rhythm this is ~0% (Fig. 1), because true ED occurs at or between frames 8 and 1.
2. % wall thickening = % [(greatest − least)/least] maximum myocardial counts per frame of the 8 R-wave intervals. This should realistically be 40%–50% for normal individuals (*17,18*) and less for patients with wall motion abnormalities.
3. % wall thickening using frame 1 = % [(greatest − frame 1)/frame 1] maximum myocardial counts, regardless of which frame actually exhibited least myocardial maximum counts. It had been hypothesized previously (*3*) that even with noticeable end-frame count losses, this quantity would provide an adequate wall-thickening estimate.

Arrhythmia Simulations

To evaluate gating error effects on cardiac parameters, standard processing was performed for group 2 patients, and then original counts per projection were altered artificially to simulate observed aberrant count patterns (Fig. 2). It was assumed that altering counts in selected R-wave intervals at certain projections for patients in normal sinus rhythm produced the same gated tomograms as would have resulted had patients actually experienced arrhythmias. Volume and EF determinations were performed separately for each simulated dataset, independent of control and ERNA EF values.

Aberrant count patterns associated with transient increases in heart rates were not simulated because these were highly variable among patients and were anticipated to be the least problematic. The three other, distinctive, gating error patterns were simulated, generating pronounced versions of each arrhythmia type (Fig. 3). Atrial fibrillation curves were altered to emulate the most severe gating error patterns observed at our institution. After alteration of original input images, all datasets were reconstructed and analyzed by perfusion and EF software. To check data-processing precision, all control data were reconstructed, and perfusion measurements were independently redetermined several months after initial computations.

Statistical Analysis

Numerical results are reported as mean values ± 1 SD. Contingency table analysis was used to compare ECG-proven arrhythmias and gating errors detected visually from tomographic curves and to evaluate agreement between algorithmic and visual gating error detection. If any contingency table entry contained less than 5 patients, log-likelihood ratio analysis was used; otherwise, χ^2 analysis was used (*19*). Cohen's kappa statistic (*20*) and Cramer's V (*19*) were computed for these tables. Unpaired *t* tests were used to compute two-tailed probabilities (*P*) that measurements were different among group 1 arrhythmias. Single-factor analysis of variance (ANOVA) was used to determine differences in quantified indices among group 2 control and simulation computations, for which $P < 0.05$ was considered statistically significant. Paired *t* tests were applied to multiple group comparisons if significance was determined by ANOVA (*20*). Linear regression was used to evaluate correlation of gated SPECT EF to mid-HLA percentage systolic count increase for group 1 patients, because EF should depend on both myocardial wall motion and thickening, with the latter presumed to be proportional to percentage systolic count increase (*9*). Linear regression analysis also was used to assess correlations between group 2 control and simulation volumes and EFs and ERNA EFs and was performed on Bland-Altman graphs of differences plotted versus averages for paired values to uncover trends and systematic errors (*21,22*). Statistical significance of two different regression results was assessed by the Fisher z test. EF changes are reported in terms of EF units.

RESULTS

For group 1 patients, 224 (59%) had no perfusion defects, and 155 (41%) had perfusion abnormalities, of whom 115 (74%) had reversible defects. Gated SPECT EF was 58% ± 14%. Arrhythmias detected by ECG monitoring during stress correlated strongly ($P < 10^{-3}$) with those detected by visual curve examination (Table 1), and Cramer's $V > 0.25$ indicated "strong" agreement (*19*). However, the low κ value of 0.18 indicated significantly more gating errors were detected by curve analysis than by ECG monitoring, probably because the former was assessed from data acquired at rest whereas the latter was performed during stress testing. Algorithms for automatically detecting aberrant count patterns agreed strongly ($P < 10^{-6}$) with observers' visual judgments (Table 2), and the κ value of 0.60 verified agreement was "excellent" (*20*). That more patterns were declared abnormal by the algorithm than by observers was likely due to a higher subjective "threshold" used by observers in defining abnormalities.

Group 1 aberrant count patterns are listed in order of ascending end-frame count loss in Table 3. Count change parameters were significantly larger than control for all detected arrhythmias, including the mildest type of gating errors associated with transient increase in heart rate (Table 3). Wall thickening was significantly less if computed using frame 1 for every gating error type. Patients in atrial fibrillation had the lowest EFs, yet these same patients also had the largest percentage of systolic count increase, twice that of patients in sinus rhythm (Table 3). This is counterintuitive, because patients with diseases should have reduced, not increased, myocardial wall thickening.

TABLE 1
Agreement Between Electrocardiogram (ECG) Monitoring and Curve Count Abnormalities

		Curve abnormalities from projection curves	
		No	Yes
ECG-demonstrated arrhythmias	No	109	59
	Yes	4	14

Log-likelihood $G^2 = 12.3$; $P < 5 \times 10^{-4}$; n = 186; degrees of freedom = 1; Cramer's V = 0.26; Cohen's κ = 0.18.

TABLE 2
Agreement Between Algorithmic and Visual Error Observations

		Gating error detected by algorithm	
		No	Yes
Gating error detected visually	No	212	9
	Yes	57	86

Odds ratio = 36:1; $P < 10^{-6}$; $\chi^2 = 138.6$; degrees of freedom = 1; Cramer's V = 0.62; Cohen's $\kappa = 0.60$.

Linear regression analysis of wall thickening versus EF demonstrated a significant correlation for group 1 patients in sinus rhythm, but not for all group 1 patients considered together (Fig. 4). Correlation for all patients was significantly weaker ($P < 0.03$) than for patients in sinus rhythm (Fig. 4). Hence, the connection between EF and percentage of systolic count increase was disrupted by gating errors.

Group 2 patients were predominately (93%) those with severe (severity 507 ± 469), extensive (extent 107 ± 76) fixed perfusion defects, abnormally low EF (42% ± 13%) and large volumes (end-diastolic volume [EDV] 134 ± 61 mL). In processing EFs, ED and ES frames had to be changed 5% of the time for control and consistently variable heart rates, in agreement with previous findings (*13*), but 22% of ectopic beats simulations and 78% of atrial fibrillation simulations. Thus, gating errors disassociated ventricular shapes from counts.

Ventricular volumes, EF, extent and severity were not significantly different among control and simulation values by ANOVA. However, individual differences for perfusion indices were large, especially for atrial fibrillation (Table 4). All perfusion score changes from control were significantly larger than processing reproducibility of control differences of extent (1% ± 24%) and severity (3% ± 28%). This occurred even for consistently variable heart rates and ectopic beats, probably because of changes in relative contributions of frames at different parts of the R-R interval in forming summed tomograms. The greatest perfusion alterations were produced by atrial fibrillation, because this generated randomly decreased amounts of summed counts at different projections, providing the backprojector with inconsistent information (*7,8*). Three control patients designated "normal" by quantitative analysis (*12*) became "abnormal," and 3 "abnormal" control patients became "normal." Whether a perfusion pattern shifted toward becoming more or less abnormal depended on diverse factors, including baseline control perfusion extent and severity and spatial distribution.

For group 2, EF and volume changes from control were negligible (Table 4), consistent with previously reported processing reproducibility (*13*). Linear correlation was strong among all simulated arrhythmia and control EFs and volumes ($r = 0.96$). Control and simulated arrhythmia EFs correlated similarly with ERNA EFs (Table 5) and were consistent with previous reports (*2,13*), with no differences ($P < 10^{-6}$) among linear correlations. Mean gated SPECT EFs were similar to one another but significantly lower than ERNA EF = 46% ± 10% by 3%–4%, consistent with previous reports that data sampling with only 8 frames compared with higher ERNA sampling rates (24–36 frames/R-R) causes EF to be underestimated by ~4% (*2,3,13,23,24*). Bland-Altman analyses (Table 5 and Fig. 5) showed lowest gated SPECT EFs underestimated ERNA EFs the most, and similarly ($P < 10^{-6}$) for all simulations. Plotting arrhythmia-induced changes from control of end-systolic volume (ESV) versus EDV (Fig. 6) demonstrated volume parameters were altered in tandem. Hence, because EF = 1 − (ESV/EDV), volume changes canceled, resulting in negligible EF change. The use of individually normalized frames (*2,13*) therefore appeared to succeed in minimizing the impact of gating errors.

Count change parameters for all group 2 simulations were significantly ($P < 10^{-6}$) larger than control values (Table 6), analogous to findings within group 1 (Table 3), and were significantly above the upper range of normal for realistic

TABLE 3
Prevalence and Count Change Parameter Characterization by Gating Error Type

Type	n	Prev	% CI	% $CI_{(1)}$	% Loss	% EF
Sinus	100	26%	32 ± 12	28 ± 10	1 ± 3	61 ± 12
TI	123	32%	39 ± 16*	31 ± 10*†	4 ± 5*	57 ± 13
CV	91	24%	56 ± 30*	33 ± 12*†	11 ± 9*	56 ± 7
EB	30	8%	62 ± 52*	38 ± 40*†	12 ± 11*	62 ± 9
AF	35	9%	64 ± 48*	29 ± 37†	16 ± 10*	46 ± 20*

*Significantly different from sinus.

†Significantly smaller than % CI within each gating error type.

Prev = prevalence; % CI = % systolic count increase; % $CI_{(1)}$ = % systolic count increase on the basis of cinematic frame 1; % Loss = % count difference between the first and last cinematic tomographic frame; % EF = % ejection fraction; Sinus = no gating error; TI = transient increase in heart rate; CV = consistently variable beats; EB = ectopic beats; AF = atrial fibrillation.

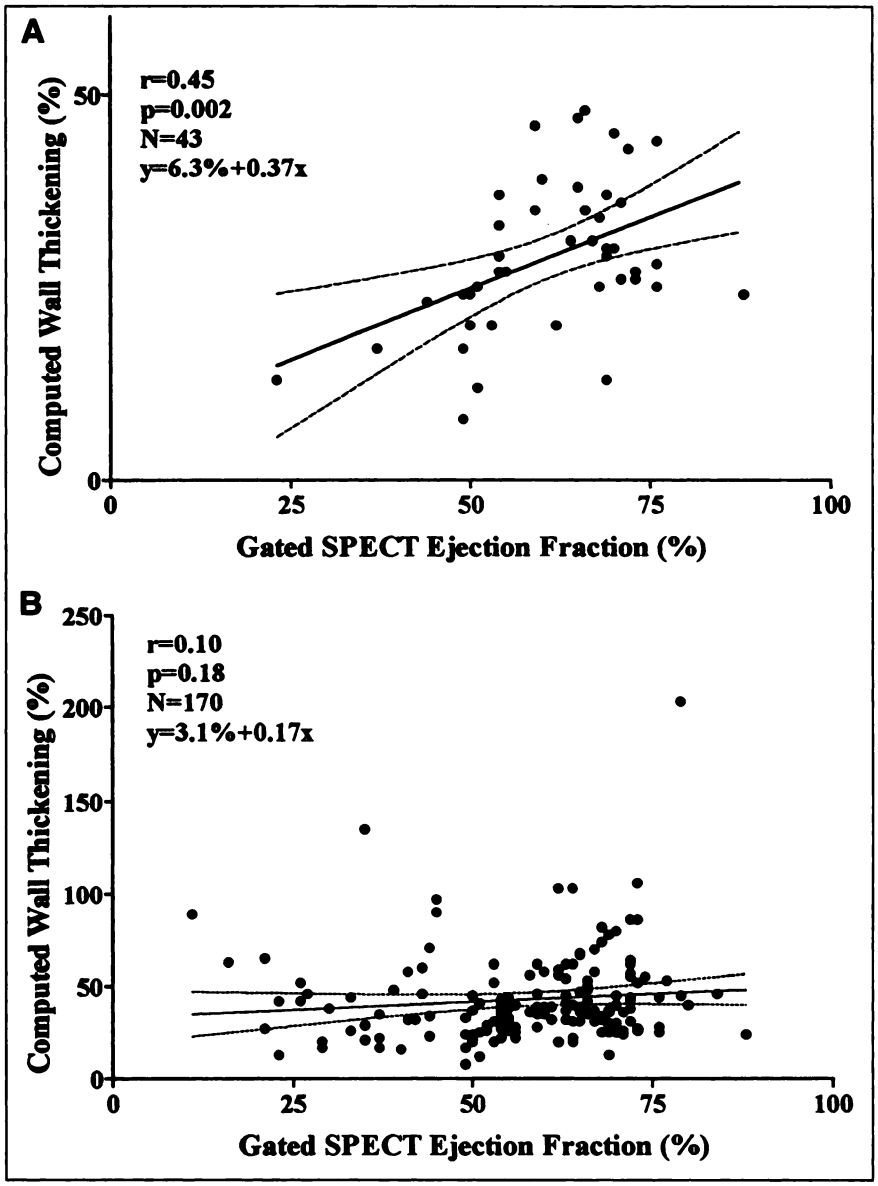

FIGURE 4. Linear regression graphs of mid-LV HLA computed wall thickening versus gated SPECT EF for patients in sinus rhythm (A) and all patients considered together (B). Graph scales for thickening range up to 210% for all patients (B) but only up to 50% for patients without gating errors (A). Also displayed are least-squares fits (solid lines) and 95% confidence limits (dashed lines).

TABLE 4
Percentage Differences of Function and Perfusion Parameters from Control Measurements by Gating Error Type

Type	ΔEF	ΔEDV	ΔESV	ΔEXT	ΔSEV
CV	1 ± 4%	2 ± 9%	−2 ± 13%	10 ± 39%*	11 ± 39%*
EB	1 ± 4%	−2 ± 10%	0 ± 10%	13 ± 45%*	14 ± 40%*
AF	2 ± 4%	−1 ± 9%	−4 ± 11%	60 ± 299%*†	76 ± 352%*†

*Different from CV and EB by paired *t* test.

†Significantly greater than processing reproducibility limits.

ΔEF = change in ejection fraction from original control values; ΔEDV = percentage change in end-diastolic volume from original; ΔESV = percentage change in end-systolic volume from original; ΔEXT = percentage change in quantified perfusion defect size from original; ΔSEV = percentage change in severity of perfusion defect from original; CV = consistently variable beats simulation; EB = ectopic beats simulation; AF = atrial fibrillation simulation.

TABLE 5
Linear Regression Results Comparing Gated SPECT with ERNA Ejection Fractions by Gating Error Type

Type	n	r	Intercept	Slope	P	SEE	95% CL
CTRL	36	0.89	−9.53 ± 4.53	1.11 ± 0.10	$<10^{-4}$	5.97	0.92–1.31
CV	36	0.86	−5.93 ± 5.02	1.05 ± 0.11	$<10^{-4}$	6.63	0.83–1.27
EB	36	0.85	−9.32 ± 5.58	1.12 ± 0.12	$<10^{-4}$	7.37	0.88–1.37
AF	36	0.89	−10.3 ± 4.9	1.17 ± 0.10	$<10^{-4}$	6.40	0.96–1.38
ΔCTRL	36	0.44	−14.4 ± 3.6	0.23 ± 0.08	0.007	5.46	0.07–0.40
ΔCV	36	0.37	−13.1 ± 4.2	0.21 ± 0.09	0.03	6.12	0.02–0.40
ΔEB	36	0.52	−16.8 ± 4.3	0.30 ± 0.10	0.004	6.60	0.10–0.49
ΔAF	36	0.47	−15.4 ± 3.8	0.29 ± 0.08	0.001	5.69	0.12–0.46

ERNA = equilibrium radionuclide angiography; Type = gating error type; r = Pearson's correlation coefficient; P = probability that regression slope = 0 (i.e., no association); SEE = standard error of the estimate (in EF units); 95% CL = 95% confidence limits of slope; CTRL = original control data; CV = consistently variable beats simulation; EB = ectopic beats simulation; AF = atrial fibrillation simulation; ΔCTRL = difference between original control EF and ERNA EF; ΔCV = difference between CV EF and ERNA EF; ΔEB = difference between EB EF and ERNA EF; ΔAF = difference between AF EF and ERNA EF.

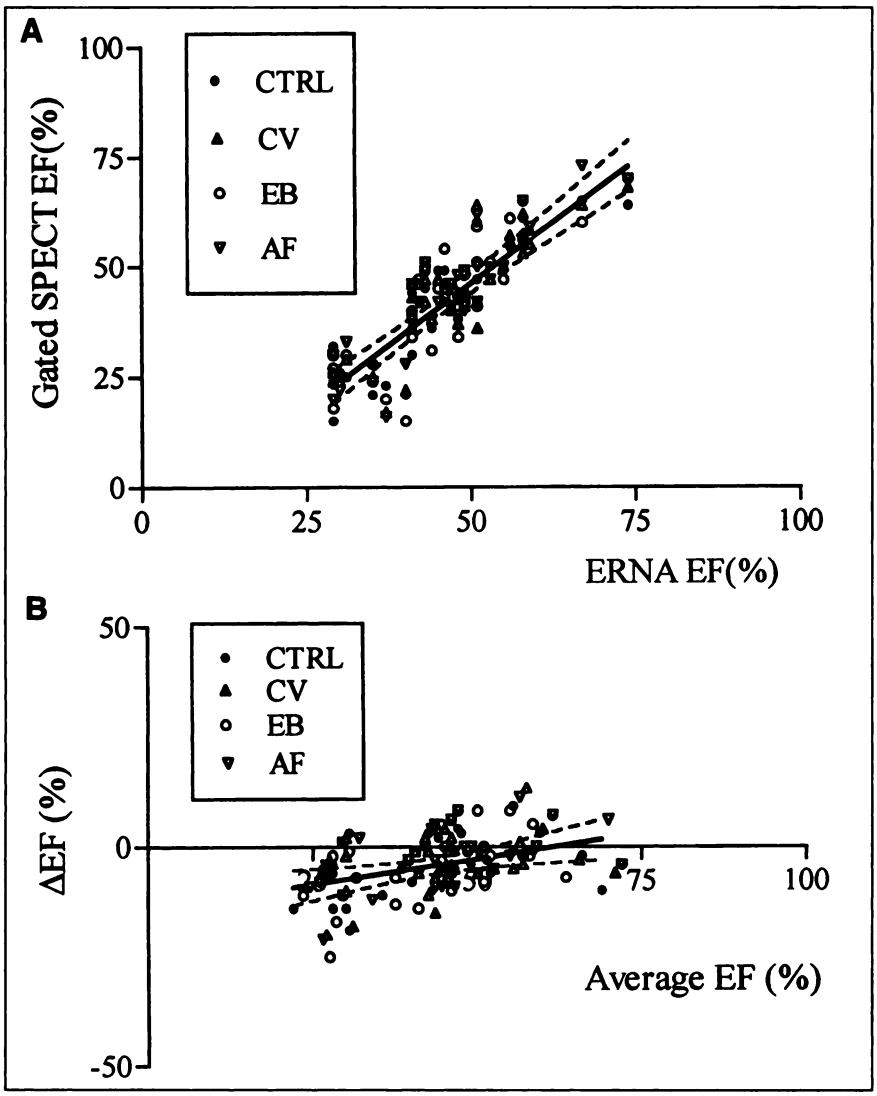

FIGURE 5. Gated SPECT EF versus ERNA EF for original control (CTRL) data and for simulations of consistently variable (CV) heart beats, ectopic beats (EB) and atrial fibrillation (AF). Linear regression graphs are shown (A), including least-squares fit of CTRL data (solid line) with 95% confidence-limiting hyperbolae (dashed lines). Associated Bland-Altman graphs are shown (B), plotting differences versus averages of gated SPECT and ERNA EFs for CTRL and simulated data.

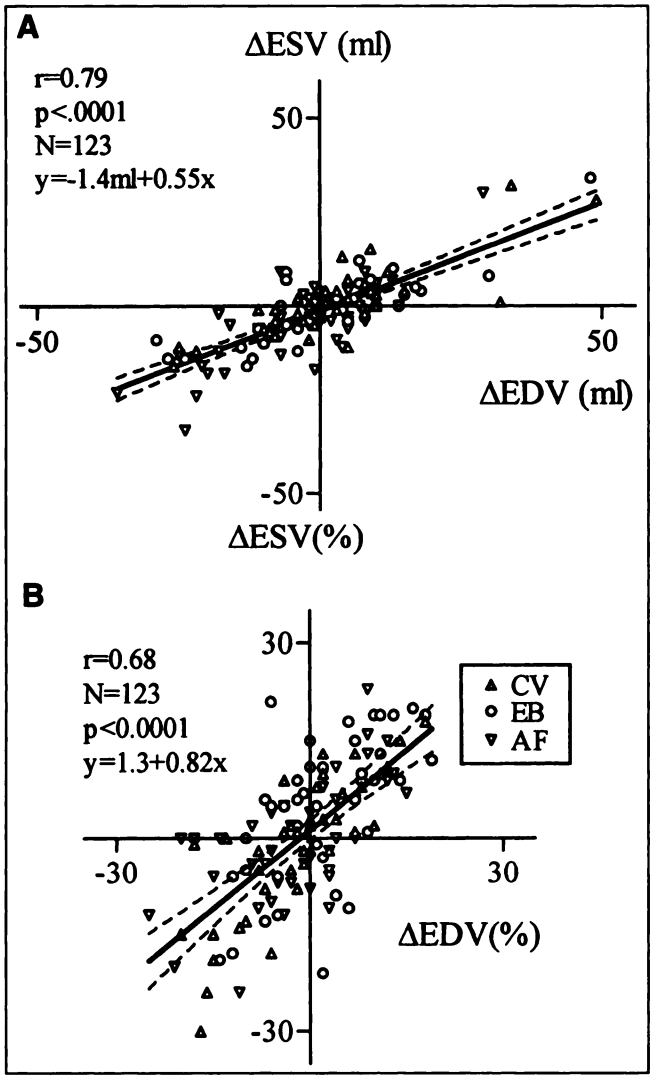

FIGURE 6. (A) Changes in milliliters between simulated arrhythmias and original control values in end-systolic volume (ΔESV) versus changes in end-diastolic volume (ΔEDV). Separate symbols are used for simulations of consistently variable (CV) heart beats, ectopic beats (EB) and atrial fibrillation (AF). Also shown is least-squares fit of all simulations for ΔESV values versus all ΔEDV values (solid lines), along with 95% confidence-limiting hyperbolae (dashed lines). (B) Percentage changes in volumes between simulated arrhythmias and original control values of end-systolic volume (ΔESV) versus changes in percentage of end-diastolic volume (ΔEDV).

myocardial thickening values of 40%–50% (*17,18*). The most sensitive measurements to gating errors were for wall thickening, probably because each class of error deprived later intervals of increasingly greater amounts of counts. Wall thickening was significantly smaller if computed using frame 1 and different from control values (Table 6). Thus, ignoring counts of the last cinematic frame in defining thickening did not provide a reliable substitute for percentage of systolic count increase in the presence of arrhythmias.

DISCUSSION

Accuracy of wall thickening and EF is of concern in the presence of gating errors because these produce alterations in systolic count increases. Wall thickening should equal systolic count increases (*9*), because myocardial walls rarely exceed typical Anger cameras' spatial resolution (*25,26*), but this is not the case if there are gating errors. All gated SPECT EF algorithms are hybrid methods that depend in varying degrees on both geometrical and percentage of systolic count increase assumptions (*2,3,13,23,27–31*). Recognizing this, some EF methods have sought to minimize arrhythmia effects by excluding the last frame from consideration (*3*), but this investigation found this precaution to be inadequate, insofar as thickening was significantly different if computed using frame 1. Also, gated SPECT images sometimes are time averaged to reduce noise levels before being input to gated SPECT EF algorithms, which would propagate end-frame count losses into cinematic frames other than the last one. Furthermore, most types of gating errors involve count decreases among several cinematic frames, not only the last frame (Fig. 2). Therefore, it is important to detect gating errors to recognize the potential for inaccurate measurements in individual patient studies.

Visual examination of original summed projection cines, used to detect non–gating-related artifacts (*5,6*), demonstrate flickering for atrial fibrillation but not for consistently variable heart rates or ectopic beats. These latter arrhythmias can elude detection unless counts of all eight curves are examined, because they do not occur at the beginning or end of data acquisition (Fig. 2). Mid-LV gated tomographic cines demonstrate progressive "dimming" of late R-wave intervals for all arrhythmia types. Deciding whether these constitute serious errors can be determined from quality assurance screens (Fig. 1); if end-frame count loss >10%, it is likely thickening calculations are incorrect (Tables 3 and 6). Fortunately, the detection algorithms described previ-

TABLE 6
Count Change Parameters by Simulated Gating Error Type

Type	% CI	% $CI_{(1)}$	% Loss
CTRL	38 ± 17%	26 ± 9%*†	5 ± 5%
CV	108 ± 21%‡	41 ± 9%*†‡	32 ± 4%‡
EB	64 ± 20%‡	20 ± 7%*†‡	16 ± 5%‡
AF	83 ± 20%‡	36 ± 8%*†‡	24 ± 6%‡

*% $CI_{(1)}$ significantly different from CTRL % CI by paired *t* test.

†% $CI_{(1)}$ significantly smaller than % CI within each gating error type.

‡Significantly different from CTRL.

Type = gating error type; % CI = percentage systolic count increase; % $CI_{(1)}$ = percentage systolic count increase based on cinematic frame 1; % Loss = percentage count difference between first and last cinematic tomographic frame; CTRL = original control data; CV = consistently variable beats simulation; EB = ectopic beats simulation; AF = atrial fibrillation simulation.

ously can discern gating errors in original projection data, so that it can be determined whether a serious arrhythmia occurred during data acquisition before the patient leaves the imaging table. For pronounced arrhythmias, an additional ungated tomogram should be acquired to obtain reliable perfusion data. If it is known beforehand that serious arrhythmias may occur, data can be acquired in gated list mode (*32*), thereby allowing the maximum latitude in reformatting data after acquisition.

Limitations of the Study

Results found in this investigation were specific to two major variables: the manner in which data were acquired, and the software used to derive quantitative parameters. The particular hardware and software used for data acquisition, and the algorithms used to compute EFs (*2,13*) and perfusion (*12*), undoubtedly influenced the results of this investigation. Different manufacturers' computer systems, using different criteria for beat rejection, may produce somewhat different acquired datasets when presented with the same patient experiencing an arrhythmia (*33–35*). It is impossible to foresee in detail the outcome of other software packages before testing them with data contaminated by gating errors, but it is plausible that atrial fibrillation causes the greatest errors, overestimating thickening, thereby potentially leading to incorrectly small ES volumes and incorrectly large EFs for those algorithms that rely most heavily on percentage of systolic count increase values.

The assumption that artificially reducing image counts simulated patients experiencing arrhythmias is an approximation. Actual volume changes for patients entering arrhythmic states, such as increased EDV accompanying atrial fibrillation, were not simulated in this study. Thus, the EF stability found in this investigation, while verifying the original software design concept of minimizing errors due to arrhythmic count changes (*2,13*), is an oversimplification. Testing more thoroughly the response of gated SPECT software to arrhythmias will require a more complicated, realistic rendering of cardiac response to aberrant electrical conduction patterns, exceeding the capabilities of the most sophisticated models used to date to evaluate gated SPECT software (*36*).

The effects of gating errors addressed by this investigation were limited to quantified variables. Although this has demonstrated the potential for incorrect calculations, arrhythmic effects on visual readings have not been studied. It will be important to document whether perfusion changes induced by arrhythmias are clinically important. Previous studies have shown that sestamibi gated tomography yields images that provide a similar impression of regional wall motion when compared with ECGs in largely normal patient populations (*37*), and even in severely hypoperfused patient populations if these latter datasets are regionally enhanced (*38*). However, gating errors could interfere with the ability of observers to discern subtle regional wall motion abnormalities from gated SPECT images.

CONCLUSION

Being able to infer myocardial wall thickening from systolic count changes is an important feature of scintigraphic gated tomograms, unique among cardiac imaging modalities, but without adequate quality assurance of gating, it may be fallacious to rely on count change information. Consequently, quality control of gating is as important as all other types of image quality assurance for the optimal derivation of accurate cardiac parameters from gated tomograms.

ACKNOWLEDGMENTS

This study was presented in part in June 1998 at the annual scientific meeting of the Society of Nuclear Medicine in Toronto, Ontario, Canada. This study was supported in part by grants from General Electric Medical Systems, Inc., Milwaukee, WI. We thank Helene Salensky for invaluable assistance in the processing of computer data.

REFERENCES

1. Grucker D, Florentz P, Oswald T, Chambron J. Myocardial gated tomoscintigraphy with Tc-99m-methoxy-isobutyl-isonitrile (MIBI): regional and temporal activity curve analysis. *Nucl Med Commun.* 1989;10:723–732.
2. DePuey EG, Nichols KJ, Dobrinsky C. Left ventricular ejection fraction assessed from gated technetium-99m-sestamibi SPECT. *J Nucl Med.* 1993;34:1871–1876.
3. Germano G, Kiat H, Kavanaugh PB, et al. Automatic quantification of ejection fraction from gated myocardial perfusion SPECT. *J Nucl Med.* 1995;36:2138–2147.
4. Mochizuki T, Murase K, Tanaka H, Kohdoh T, Hamamoto K, Tauxe WN. Assessment of left ventricular volume using ECG-gated SPECT with technetium-99m-MIBI and technetium-99m-tetrofosmin. *J Nucl Med.* 1997;38:53–57.
5. DePuey EG, Rozanski A. Using gated technetium-99m-sestamibi SPECT to characterize fixed myocardial defects as infarct or artifact. *J Nucl Med.* 1995;36:952–955.
6. DePuey EG. Artifacts in SPECT myocardial imaging. In: DePuey EG, Berman DS, Garcia EV, eds. *Cardiac SPECT Imaging*. New York, NY: Raven Press; 1995:169–200.
7. Nichols K, Galt JR. Quality control for SPECT imaging. In: DePuey EG, Berman DS, Garcia EV, eds. *Cardiac SPECT Imaging*. New York, NY: Raven Press; 1995:21–48.
8. King MA, Xia W, deVries DJ, et al. A Monte Carlo investigation of artifacts caused by liver uptake in single-photon emission computed tomography perfusion imaging with technetium-99m-labeled agents. *J Nucl Cardiol.* 1996;2:18–29.
9. Galt JR, Garcia EV, Robbins WL. Effects of myocardial wall thickness of SPECT quantification. *IEEE Trans Med Imaging.* 1990;9:144–150.
10. DePuey EG, Nichols KJ, Slowikowski JS, et al. Fast stress and rest acquisitions for technetium-99m-sestamibi separate-day SPECT. *J Nucl Med.* 1995;36:569–574.
11. Crawford CR. CT filtration aliasing artifacts. *IEEE Trans Med Imaging.* 1991;10:99–102.
12. Van Train KF, Areeda J, Garcia EV, et al. Quantitative same-day rest-stress technetium-99m-sestamibi SPECT: definition and validation of stress normal limits and criteria for abnormality. *J Nucl Med.* 1993;34:1494–1502.
13. Nichols K, DePuey EG, Rozanski A. Automation of gated tomographic left ventricular ejection fraction. *J Nucl Cardiol.* 1996;3:475–482.
14. Tortoledo FA, Quinones MA, Fernandez GC, Waggoner AD, Winters WL. Quantification of left ventricular volumes by two-dimensional echocardiography: a simplified and accurate approach. *Circulation.* 1983;67:579–584.
15. Reiber JHC, Lie SP, Simoons ML, et al. Clinical validation of fully automated computation of ejection fraction from gated tomographic equilibrium blood-pool scintigrams. *J Nucl Med.* 1983;24:1099–1107.
16. Christian PE, Nortmaan CA, Taylor A. Comparison of fully automated and manual ejection fraction calculations: validation and pitfalls. *J Nucl Med.* 1985;26:775–782.

17. Sechtem U, Sommerhoff BA, Markiewicz W, White RD, Cheitlin MD, Higgins CB. Regional left ventricular wall thickening by magnetic resonance imaging: evaluation in normal persons with global and regional dysfunction. *Am J Cardiol.* 1987;59:145–151.
18. Clausen M, Bice AN, Civelek AC, Hutchins GM, Wanger HN Jr. Circumferential wall thickness measurements of the human left ventricle: reference data for thallium-201 single-photon emission computed tomography. *Am J Cardiol.* 1986;26:827–831.
19. Agresti A. *Categorical Data Analysis.* New York, NY: John Wiley; 1990.
20. Zar JH. *Biostatistical Analysis.* Englewood Cliffs, NJ: Prentice-Hall; 1984.
21. Bland JM, Altman DG. Statistical methods for assessing agreement between two methods of clinical measurement. *Lancet.* 1986;1:307–310.
22. Bland JM, Altman DG. A note on the use of the interclass correlation coefficient in the evaluation of agreement between two methods of measurement. *Comput Biol Med.* 1990;20:337–340.
23. Cooke CD, Garcia EV, Cullom SJ, Faber TL, Pettigrew RI. Determining the accuracy of calculating systolic wall thickening using a fast Fourier transform approximation: a simulation study based on canine and patient data. *J Nucl Med.* 1994;35:1185–1192.
24. Nichols K, Tamis J, DePuey EG, Mieres J, Malhotra S, Rozanski A. Relationship of gated SPECT ventricular functional parameters to angiographic measurements. *J Nucl Cardiol.* 1998;5:295–303.
25. Nichols K, DePuey EG, Rozanski A, Salensky H, Friedman MI. Image enhancement of severely hypoperfused myocardia for computation of tomographic ejection fraction. *J Nucl Med.* 1997;38:1411–1417.
26. Nichols K, DePuey EG, Friedman MI, Rozanski A. Do patient data ever exceed the partial volume limit in gated SPECT studies? *J Nucl Cardiol.* 1998;5:484–490.
27. Buvat I, Bartlett ML, Kitsiou AN, Dilsizian V, Bacharach SL. A "hybrid" method for measuring myocardial wall thickening from gated PET/SPECT images. *J Nucl Med.* 117;38:324–329.
28. Faber TL, Akers MS, Peshock RM, Corbett JR. Three-dimensional motion and perfusion quantification in gated single-photon emission computed tomograms. *J Nucl Med.* 1991;32:2311–2317.
29. Smith WH, Kastner RJ, Calnon DA, Segalla D, Beller GA, Watson DD. Quantitative gated single photon emission computed tomography imaging: a counts-based method for display and measurement of regional and global ventricular systolic function. *J Nucl Cardiol.* 1997;4:451–463.
30. Calnon DA, Kastner RJ, Smith WH, Segalla D, Beller GA, Watson DD. Validation of a new counts-based gated single photon emission computed tomography method for quantifying left ventricular systolic function: comparison with equilibrium radionuclide angiography. *J Nucl Cardiol.* 1997;4:464–471.
31. Williams KA, Taillon LA. Reversible ischemia in severe stress technetium-99m-labeled sestamibi perfusion defects assessed from gated single-photon emission computed tomographic polar map Fourier analysis. *J Nucl Cardiol.* 1995;2:199–206.
32. Gelfand MJ, Thomas SR. Acquisition and processing—two-dimensional studies. In: Gelfand MJ, Thomas SR, eds. *Effective Use of Computers in Nuclear Medicine.* New York, NY: McGraw-Hill; 1988:1–30.
33. Cullom JS, Case JA, Bateman TM. Electrocardiographically gated myocardial perfusion SPECT: technical principles and quality control considerations. *J Nucl Cardiol.* 1998;5:418–425.
34. Bacharach SL, Bonow RO, Green MV. Comparison of fixed and variable temporal resolution methods for creating gated cardiac blood pool image sequences. *J Nucl Med.* 1990;31:38–42.
35. Juni JE, Chen CC. Effects of gating modes on the analysis of left ventricular function in the presence of heart rate variation. *J Nucl Med.* 1988;29:1272–1278.
36. Achtert AD, King MA, Dahlberg ST, Pretorius PH, LaCroix KJ, Tsui BMW. Investigation of the estimation of ejection fractions and cardiac volumes by a quantitative gated SPECT software package in simulated gated SPECT images. *J Nucl Cardiol.* 1998;5:144–152.
37. Chua T, Kiat H, Germano G, et al. Gated technetium-99m sestamibi for simultaneous assessment of stress myocardial perfusion, post exercise regional ventricular function and myocardial viability. *J Am Coll Cardiol.* 1994;23:1107–1114.
38. Nichols K, DePuey EG, Krasnow N, Lefkowitz D, Rozanski A. Reliability of enhanced gated SPECT in assessing wall motion of severely hypoperfused myocardia: an echocardiographic validation. *J Nucl Cardiol.* 1998;5:387–394.